

Original Article

Near-surface geophysical investigation in Mae On, Chiang Mai, Thailand

Siriporn Chaisri^{1*}, Srivipa Lerkrattanawaree², Niti Mankhemthong²,
Suwimon Udphuay², and Mingkhwan Kruachanta²

¹ *Department of Physics and Materials Science, Faculty of Science,
Chiang Mai University, Mueang, Chiang Mai, 50200 Thailand*

² *Department of Geological Sciences, Faculty of Science,
Chiang Mai University, Mueang, Chiang Mai, 50200 Thailand*

Received: 17 May 2019; Revised: 10 August 2019; Accepted: 18 September 2019

Abstract

The objective of this study is to map a sedimentary layer overlying volcanic basement in Mae On area, Chiang Mai, Thailand. Seismic reflection, multichannel analysis of surface waves and electrical resistivity surveys were conducted to provide additional supporting information in the shallow part of subsurface geometry. The deeper part information is evaluated from the previous magnetic and gravity anomaly maps. The interpretation from seismic reflection is used to constrain gravity forward modeling to obtain a pseudo-geological model. The final model presents that there are a thin Quaternary sediment layer with low electrical resistivity and seismic velocity, overlies volcanic basement with high electrical resistivity and high seismic velocities. The volcanic basement can be recognized as a heterogeneous body with horizontally characteristic layers of volcanic flows based on seismic reflection profiles. The volcanic basement underneath the sediment layer shows a high anomaly on gravity and magnetic maps.

Keywords: Mae On, seismic reflection, MASW, electrical resistivity, gravity model

1. Introduction

Mae On district is about 40 km to the east of Chiang Mai City center, northern Thailand. Its geomorphology is considered as a valley, which is 3 kilometers wide and 13 kilometers long, bounded by topographic high terrains to the west and east. The valley is mostly covered by Quaternary sediments related to recent fluvial and alluvial processes and located in the foothill terrain with a long shape in north-south trend (Department of Mineral Resources, 2007) (Figure 1). The western side of the study area is Permian volcanic rocks (Wang *et al.*, 2017) and Carboniferous sandstone (Hara *et al.*, 2017), while the eastern side is Silurian-Devonian meta-

sedimentary rocks. The volcanic rocks in the study area were assigned to be a part of the Chiang Mai-Chiang Rai Suture Zone, Metcalfe (2017). Field survey and petrography by Barr and Cooper (2013); Barr, Tantisukrit, Yaowanoyothin, and Mac Donald (1990); Phajuy, Panjasawatwong, and Osataporn (2005), described that types of the volcanic rocks are the Permian tuff and basalt units composed of green tuff, gray to dark green basaltic flows, hyaloclastite, pyroclastic and pillow breccia. There are also the potential field data available from the Department of Mineral Resources (DMR, 2015) including the regional gravity data covered the northern part of Thailand conducted in 2015 and the aeromagnetic data which were a part of the nationwide aeromagnetic grid (Hatch *et al.*, 1994). The regional gravity data were collected as random points on the ground surface with spacing about 1 kilometer. The data were deducted by a conventional procedural using 2.67 g/cm³ Bouguer density with terrain correction for the complete Bouguer gravity anomaly map with 500 meters grid spacing.

*Corresponding author

Email address: siriporn.chaisri@cmu.ac.th

The aeromagnetic data were collected with 1-kilometer line spacing in N-S direction and the sensor height about 762 meters (2500 feet) mean terrain clearance (MTC). The data were processed to generate the residual magnetic map with a grid cell size of 500 meters and at 300 meters mean terrain clearance. The reduction to the Pole (RTP) was applied to take out the effect of geomagnetic field inclination. Figure 2 displays the complete Bouguer gravity map and the RTP of the residual magnetic map in the study area cropped from the regional maps. Both maps show high anomalies in the study area. However, in general, sedimentary unit should provide low anomalies of gravity and magnetic maps because of their low density and low magnetic susceptibility. There are also basalt outcrops distribute in this area. Additionally, there is also a well-log data available from DMR (Department of Mineral Resources, 2003) shown that there is a Quaternary sediment layer about 80 m thick overlaying basaltic rock layer. Nevertheless, the well location (indicates by the star in Figure 1) is about 6.5 km in the southwestern direction away from the study area, as a result, some geological information might be varied especially the sedimentary thickness. Therefore, the Quaternary sediment layer in Mae On area

should be thinner and thus basaltic rock underneath influence more on gravity and magnetic maps showing high values, the possibility of a thin layer of sediment overlaying basalt layer. To verify these contradictories, more information is needed such as geophysical data from seismic and electrical resistivity surveys for revealing the shallow subsurface geometry underneath Mae On area. Therefore, the purpose of this study is to map the Quaternary layer using 4 different geophysical methods. The 2-D forward modeling of gravity data was performed to obtain a 2-D pseudo-geological model across profiles AA' in Figure 2 with initial information of shallow Quaternary sediment from seismic reflection, multichannel analysis of surface wave (MASW) and electrical resistivity tomography (ERT) surveys. The previous magnetic and gravity anomalies maps were analyzed to provide more information on the deeper part. However, the aeromagnetic data are not yielded for analysis in forward modeling due to the limit of data density and more complication of susceptibility value. The probable geological model will be proposed based on gravity data analysis combine with the results from seismic cross section and surface geological map.

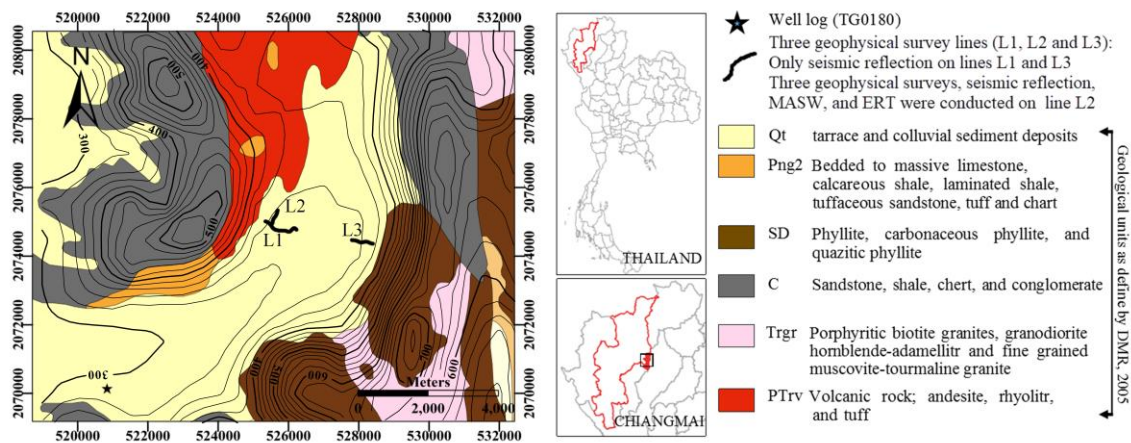


Figure 1. Geological map of Mae On area with the elevation contour interval 25 m, Chiang Mai, Thailand, black lines indicate geophysical surveys and star indicates well log location, Department of Mineral Resources (2007).

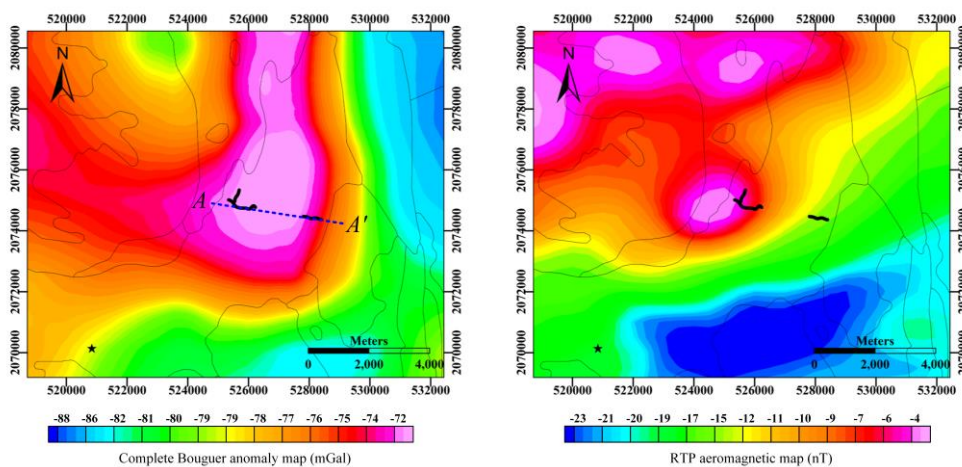


Figure 2. With outline of the geological unit, (Left) Complete Bouguer gravity anomaly map, Department of Mineral Resources (2015), dashed blue line indicates profile section AA' for gravity forward modeling and (Right) Reduction to the pole of the residual aeromagnetic map, Hatch *et al.* (1994), in the Mae On area.

2. Field Surveys

This study includes four geophysical methods, reflection seismic methods focused on seismic body waves, multichannel analysis of surface wave method focused on surface waves, electrical resistivity method studied the electrical property of subsurface materials, and gravity forward modeling to determine a 2-D geological model. There are three selected geophysical survey lines (Figure 1) for this study. Two survey lines, L1 and L3 in the east-west direction, were investigated with reflection seismic method with surface distance about 1000 m and 580 m, respectively. Survey line L2, approximately in the north-south direction, was investigated by seismic reflection and resistivity surveys with surface distance about 460 m. The application of surface wave from MASW method was also conducted in the middle part of line L2.

2.1 Seismic reflection survey

The seismic reflection method focuses on the velocity of reflected wave. Their hyperbolic travel time curves are used to estimate velocity in data processing and construct the structure velocity model. It is utilized to create a pseudo-geological model by combination with other geophysical data. The seismic reflection surveys were conducted with three Geode Geometrics DZ systems, a total of 72 channels per shot with 28 hertz frequency respond geophones. The acquisition along survey line L1 was done by using a 300 kilograms elastic wave generator (EMG) as a seismic source with the original target depth to the bottom of basaltic layer. After analyzing the shot record, the first arrival times show the existence of a very high P-wave velocity at a very shallow location and the seismic wave could only penetrate in an upper shallow zone (Figure 3a). Therefore, we decided to investigate furthermore by using a 9-kg sledgehammer as a seismic source instead to decrease the survey cost. The survey line L2 was selected for investigating the orientation of the subsurface layer in north-south direction. Due to a limitation of the survey location, the seismic reflection survey could not be done across the study area, then the survey L3 located at the east side of the study area was selected with the similar subsurface geometry assumption. Three or five shots were

generated and vertically stacked for each shot location to increase the signal-to-noise ratio (S/N) with 0.5 milliseconds sampling time interval and 1 second total time record. For survey line L1 and L2, shot and geophone intervals equal to 4 meters with approximate 2 meters bin size processing and a total of 515 and 230 CMP numbers, respectively. After field parameter testing on L3, it showed the similar structure to that from survey line L1 and L2. Therefore, to decrease data collecting time, we decided to use shot and geophone intervals equal to 5 meters for survey line L3, with approximate 2.5 meters bin size processing and a total of 240 CMP numbers.

Seismic field records were analyzed and processed with Vista5.5 seismic reflection data processing software. The effect of using different source can be distinguished by the frequency content of the seismic data. The example of shot record in Figure 3a, using EWG as seismic source, has a lower dominant frequency than that in Figure 3b and Figure 3c which using a 9-kg sledgehammer as seismic source. This is because the EMG has approximately 2 times of the ground impact areas (30x30 square centimeters) bigger than that of the metal plate used for the sledgehammer. The lower frequency content leads to the lower vertical resolution but signal can travel deeper. The seismic shot gathers are inspected for ground layer velocities estimation by the first arrival times, the directed and refracted waves, Figure 3. The directed wave arrival has velocity approximately 600 m/sec assumed as the topsoil or weathering layer with a very small thickness. The refracted wave re-presented in second reciprocal slope indicates the velocity of second layer as 4,400 m/sec. The surface wave and air blast can also be indicated with an apparent velocity of about 200 meter/second and 330 meter/second respectively. The conventional reflection processing procedure is performed including elevation static, FK-filter, frequency filter, deconvolution, velocity analysis, normal moveout correction, and then stacking. The parameters for all processing procedures were tested and visualized for the best effect on noise attenuation to improve the signal to noise ratio on shot gathers. We do not perform migration because of the simple subsurface geometry expected in the area. The final stacked sections are displayed in Figure 4a and Figure 6. In Figure 6, the final seismic reflection profiles from L1 and L3 express the effect of using the different source as the lower dominant frequency of the signal in section from L1

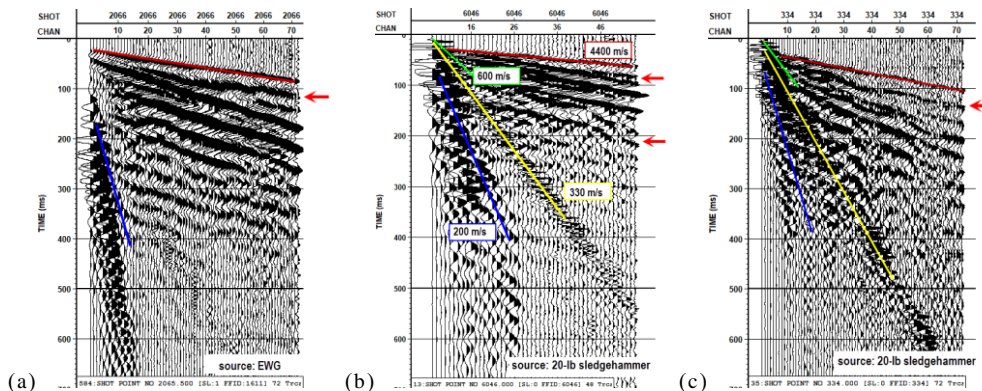


Figure 3. Selected shot records with mean scaling applied from survey line (a) L1, (b) L2, and (c) L3 showing the linear events, directed wave, air wave, refracted wave and ground roll indicated with velocity information in green, yellow, brown, and blue lines, respectively. The red arrows indicate the reflected waves.

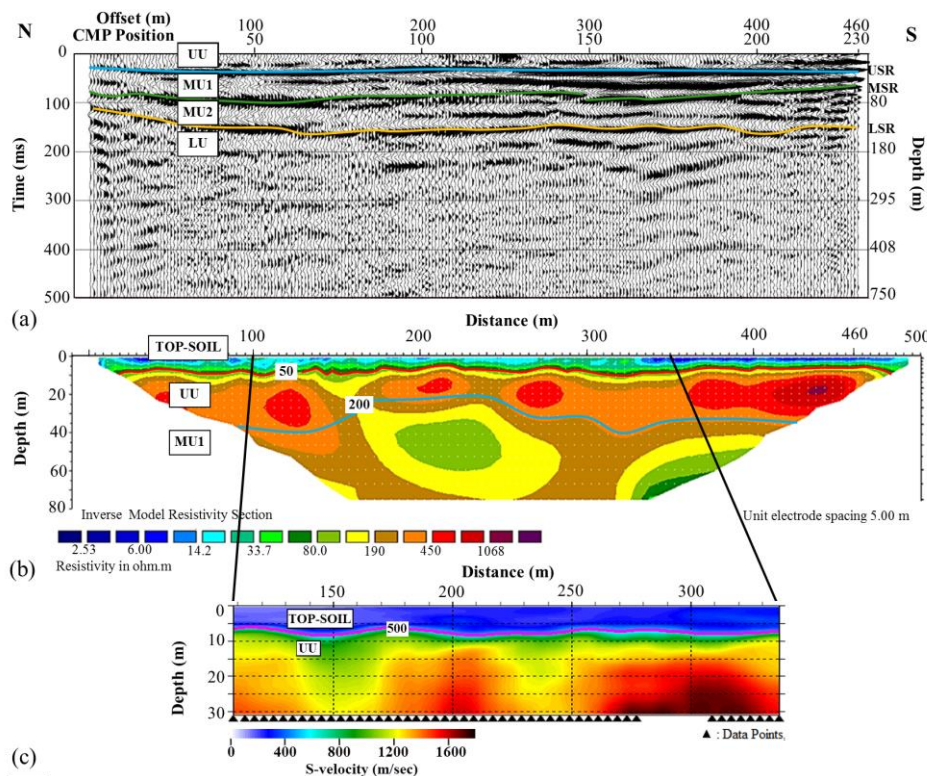


Figure 4. Results from geophysical surveys of line L2 in N-S direction (a) seismic reflection section, (b) electrical resistivity model, and (c) S-wave velocity profile from MASW method.

(EMG source). Stack section resulted from line L2 (Figure 4a) is used for interpretation with results from MASW and ERT surveys. The interpretation from stack sections of line L1 and L3 (Figure 6) are used to constrain gravity forward modeling.

2.2 Electrical resistivity tomography

To examine subsurface in terms of electrical properties, the 2-D ERT survey is performed. Electrical current is injected into the ground via a pair of electrodes and then the resulting electrical potential is measured with selected pairs of electrodes to create apparent electrical resistivity section. The separation of current and potential electrodes defines the depth of investigation, (Everett, 2013; Loke, 2018). ERT is acquired with ABEM Terrameter SAS4000 resistivity meter, on survey line L2. The dipole-dipole electrodes configuration, which has comparatively high sensitivity and very good noise rejection circuitry, is used with an electrode spacing of 5 meters. The observed apparent resistivity data undergo the inversion calculation by RES2DINV software for obtaining 2-D true electrical resistivity model. The iteration of least-squares inverse routine is applied to properly match between a field apparent resistivity and calculated apparent resistivity. Figure 4b presents 2-D electrical resistivity model cross section resulted from the inversion process with the 10 iteration calculations and final 5% RMS error.

2.3 Multichannel analysis of surface waves

MASW methods focus on surface waves that have velocity dispersion properties, which are affected by sub-

surface layering (Miller, Xia, Park, & Ivanov, 1999; Park, Miller, & Xia, 1999; Xia, Miller, & Park, 1999). In the layered earth, surface wave at different frequency is influenced by the properties of different depth zone, P-wave, S-wave velocities and density. With the increasing velocity layered earth, surface waves at low frequency travel faster. Dispersion properties of surface waves relate to seismic body wave velocity particularly S-wave velocity. To capture characteristic of surface wave dispersion, proper acquisition parameters must be utilized. MASW data acquisition used the same equipment system as seismic reflection survey but with 4.5 hertz frequency response geophones to capture more surface wave energy because of the lower frequency content of surface waves. Shot gathers for MASW are recorded with 30 channels per shot, 1 millisecond interval sampling time, 1 second total time record, 2 meters geophone spacing, 4 meters shot spacing, and 8 meters of the distance between shot location to the first geophone.

MASW data were processed with ParkSEIS[®] (v.2) for 2-D Vs profiles, Park Seismic LLC. (2018). The field records are transformed into phase velocity spectrum for dispersion analysis, Park *et al.* (1998), to estimate the fundamental mode dispersion curves. The iteration of least-squares inverse routine is applied to properly match between picked dispersion curve and calculated dispersion curve which carry out from measurement and initial model, respectively. The selected MASW shot record for analyzing the surface wave at the location 100 meters on the survey line L2 is shown in Figure 5. The solution from MASW method is the S-wave velocity profile displayed in Figure 4c.

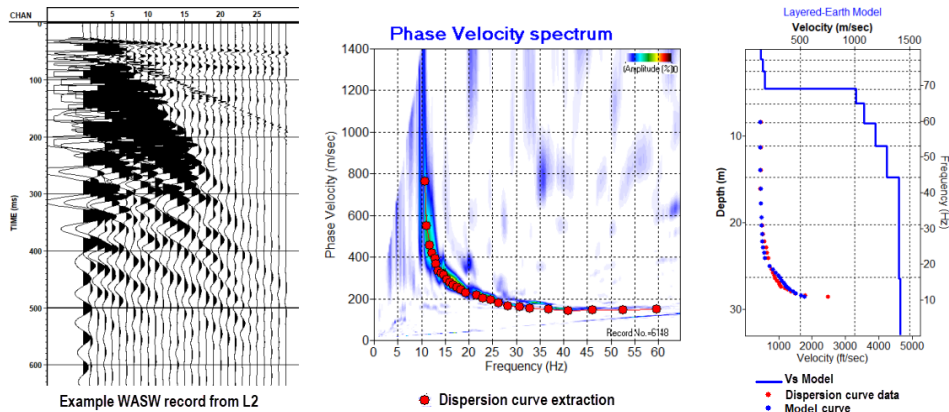


Figure 5. From left to right, the example of WASW shot record, dispersion curve extracted from phase velocity spectrum, and the Vs model solution from inversion calculation with 83.79% dispersion curve matching.

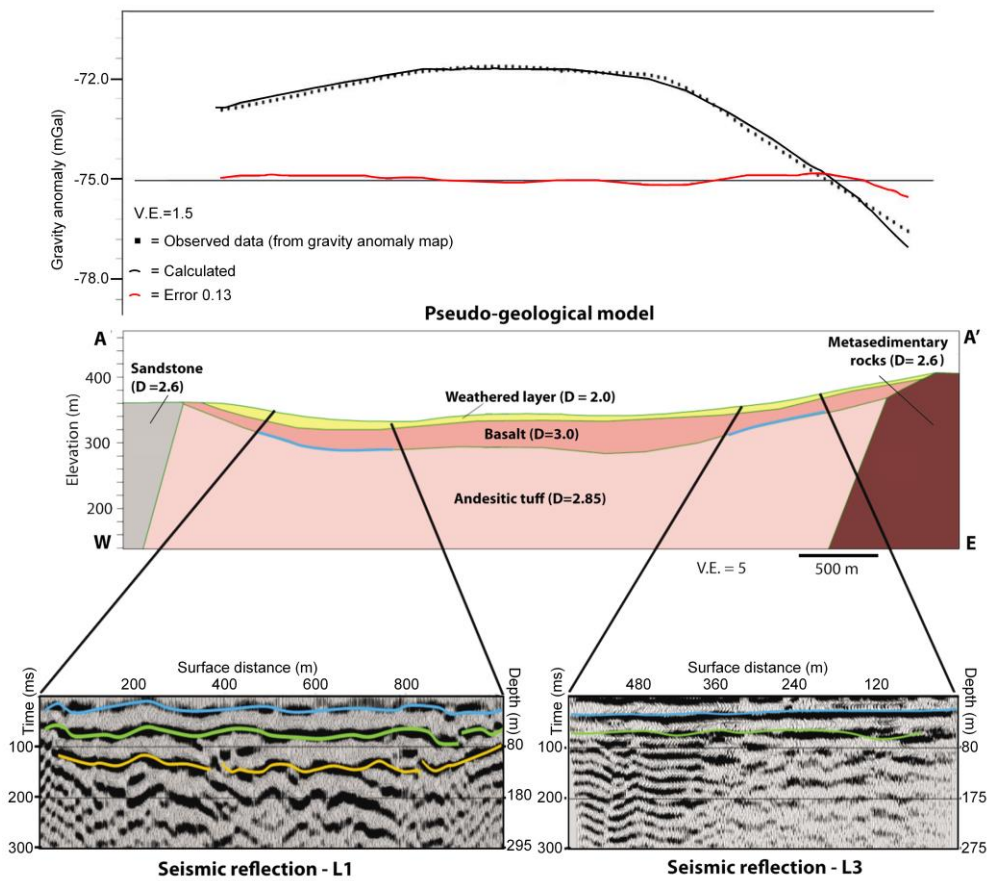


Figure 6. Pseudo-geological modeling, (top) gravity response, (middle) solution from gravity forward modeling of profile AA' constrained by seismic reflection profiles L1 and L3 (bottom).

3. Survey Results

Seismic reflection profiles, L2 (Figure 4a), L1 and L3 (Figure 6), show three main seismic reflectors. There are upper (USR), middle (MSR), and lower (LSR) reflectors that represented with blue, green, and yellow lines, respectively. The USR reflector presents the high continuity, high amplitude and nearly horizontal pattern with travel time about 35-50 milliseconds. The MSR reflector shows high amplitude,

moderate continuity, and nearly irregular pattern with travel time about 80-110 milliseconds. The deepest reflector, LSR, shows high amplitude and moderate continuity with slightly dipping to southward with 120-180 milliseconds two-way travel time. The reflector USR, MSR, and LSR separate four major seismic units. The Upper unit (UU) has an interval velocity about 1,500 m/s with a 30 m average thickness. It is underlain by the mid unit (MU) that divided into two subunits, MU1 and MU2. The top unit, MU1, has an interval velocity of

about 1,800 meter/second with an average thickness of 80 m and the lower unit, MU2, has an interval velocity 1,900 meter/second with 30 m average thickness. The Lower unit (LU) has an interval velocity higher than 2,100 meter/second.

The results from 2-D ERT and MASW surveys show the detail of the upper part geological structure. The true electrical resistivity model (Figure 4b) from line L2 displays three nearly horizontal layers with the maximum investigation depth of about 70 m. Whereas, the S-wave velocity model (Figure 4c) explores more detail of near-surface layers with the maximum investigation depth of about 30 m.

The top-soil layer defined with low electrical resistivity, less than 50 Ohm.meter, and low S-wave velocity, less than 400 meter/second, has the thickness approximately 5-10 meters which are corresponding to a low P-wave velocity of 600 meter/second (directed wave) which could not witness in seismic reflection sections. However, from the first arrival time in seismic reflection shot record, there is a shallow high P-wave velocity (about 4,400 meter/second) layer that might be corresponding to UU unit. It has an estimated thickness of 30 meters (Figure 4a) with high electrical resistivity ranging from 50 to 600 Ohm.meter (Figure 4b). The UU unit also has high S-wave velocity approximately higher than 1,800 meter/second in the southern part of line L2 (Figure 4c) which could be related to the hard rock unit. In addition, well data from the adjacent area represents sediment layer overlaying basalt layer thus there is the probability that the UU unit is a basaltic layer (Chaturong kawanich, Soponpongipat, & Chuaviroj, 1984). The deepest layer from electrical resistivity model is corresponding to MU1 unit of the seismic section has resistivity range 35-200 Ohm.meter.

Below the basaltic layer, there are MU1, MU2, and LU units from seismic cross sections (Figure 4a) that presumed as the pyroclastic layers, according to Barr and Charusiri (2011) and verified base on three reasons. The first, those layers are contacted with basalt layers, therefore, the paleoenvironment when they accumulate should not change rapidly. The second is the origin of pyroclastic deposits as a horizontal layer in each event which confirmed by the seismic reflection profiles presented as horizontal reflectors (Figure 4a and Figure 6). The third, there is the high resistivity layer which is underlying basaltic layer in electrical resistivity profile (MU1 in Figure 4b). It is consequence related to volcanic rock; however, this layer has lower resistivity value than that of the basaltic layer.

4. 2-D Gravity Forward Modeling

The purpose of the forward calculation is to acquire geophysical response by assigned earth's physical properties with earth's geometry, Blakely (1996). The 2-D gravity forward modeling is achieved using GM-SYS Geosoft Oasis Montaj software. The initial geologic cross-section model is defined based on constraint information from all geophysical methods or well data or geological survey. Before the forward calculation, the complete Bouguer anomaly map was regridded into the small spacing of 50 meters for more data points whereas the original grid size was 500 meters. Since we assume that the subsurface in study area is not that complicate, the resize of the gravity grid spacing should not have any problem. The decision of the profile AA' line selection was based on our supported geophysical data. Beyond the profile

AA' line is the area up into the high mountains, which was not accessible and where no gravity data could be collected. The profile AA' (Figure 2) crosses overlap two reflection seismic cross-sections, L1 and L3. They are used to constrain the initial depth and criteria of the pseudo-geological model in the shallow zone, upper 180 meters. From the geophysical survey results, Figure 4, the topsoil (weathered layer) has the thickness approximately 5-10 meters and the bottom of the basaltic layer is approximately 30-40 meters from the ground surface. The depth of the deeper zone is approximated by using radially average power spectrum of gravity and magnetic data. It represents the volcanic boundary at approximately 500-1000 meters depth. The western side of the study area is presumed as Carboniferous sandstone, while the eastern side is presumed as Silurian-Devonian metasedimentary rocks. The geologic cross section model is then modified interactively until an acceptable agreement is reached between calculated and observed values. Gravity forward modeling was done on the profile AA' and the final pseudo-geological model is presented in Figure 6.

Rock's Density information is the main parameter to construct a Pseudo-geological model from gravity modeling. The initial densities of rocks in this area are derived from gravity survey in the adjacent area, Chiang Mai Basin, (Wattananikorn *et al.*, 1995). Follow Wattananikorn *et al.* (1995), the density of Carboniferous sandstone and Silurian-Devonian metasedimentary rocks in this study defined as 2.60 g/cm³, and the average density of the topsoil layer is defined as 2.00 g/cm³. There is no information involving density value of volcanic rock in this area, thus the volcanic rock density is estimated from the well-known textbook, Telford *et al.* (1990). The average basalt density equal to 3.00 g/cm³ is used. The underneath basalt unit is presumed as the andesitic tuff unit (Chaturongkawanich *et al.*, 1984). Its density is estimated by the average density of the volcanic rock which is 2.85 g/cm³. For reliable and better solutions, the different type of rock samples should be collected to estimate their density and if it is possible more well-log information within the study area. Other geophysical methods including 3D gravity inversion could carry on for further investigation.

5. Discussion

Near-surface geometry could not be detected by seismic reflected wave and potential field data especially the aeromagnetic data, due to the height of data collection. There is also a lack of information on the susceptibility value of the volcanic rock in the area. Therefore, the magnetic data were used only for estimating the depth of volcanic boundary by analyzing the radially average power spectrum. The magnetic anomaly on L1 is about -6 nT and that on L3 is about -13 nT (Figure 2), whereas seismic sections show the similar subsurface structure. The higher magnetic anomaly in L1 might be the effect from the unevenly of volcanic boundary underneath or the adjacent volcanic rock unit in the northwest of the line survey, the red unit in Figure 1. Therefore, the physical properties and thickness of the topsoil layer were approximated from ERT, MASW, and seismic first arrival time methods. From the first arrival time of seismic shot record, there is a high P-wave velocity contrast between top-soil (600 m/s) and UU unit (4,400 m/s) with a very shallow interface. It causes the strong multiple reflections very near the ground

surface in seismic reflection record, less seismic energy transmitted through subsurface. This creates problems in data processing which limited only in the shallow zone because seismic energy cannot penetrate to the deeper part, seen only upper 300-400 milliseconds. In reflection seismic data processing, it is difficult to distinguish a shallow reflection event from refraction event in shot gathers. Seismic reflection method is not able to detect the thin layer of topsoil because of the vertical resolution limit. Thus, the seismic velocity of the unit above reflector USR is merged into one velocity, which is the average velocity of the lithology UU unit.

6. Conclusions

The geophysical methods have been done including seismic reflection survey, MASW, ERT, and gravity forward modeling. The previous magnetic and gravity anomalies maps were analyzed to provide more information on the deeper part. The solution from seismic profile was integrated with electrical resistivity and S-wave velocity profiles to confirm the shallow part. The interpretation from all geophysical surveys was used to constrain the gravity forward modeling to obtain the pseudo-geological model. The result shows that there is a sediment layer about 5-10 meters thick with low electrical resistivity and seismic velocity values that overlies a high electrical resistivity and seismic velocity layer which could be interpreted as a volcanic basement with an approximate depth of 500-1,000 meters. Moreover, the basement could be a basaltic layer based on basaltic outcrops in this area. Seismic cross sections show the volcanic rock is the heterogeneous body with horizontally characteristic layers of volcanic flows and pyroclastic falls. This study verifies the possibility of relatively thin layer of Quaternary sediment showing high gravity and magnetic anomaly. This sediment layer is underlined by high-density a volcanic rock.

Acknowledgements

This work was supported by the CMU Junior Research Fellowship Program, and the Science Achievement Scholarship of Thailand (SAST). We would like to thank the Department of Mineral Resources (DMR) for gravity and magnetic data. Many thanks go to the staff from Geophysics Research Laboratory at the Department of Geological Sciences, Faculty of Science, Chiang Mai University, for their assistance in fieldwork. We appreciate that our paper was selected from the 8th International Conference on Applied Geophysics, Songkhla, November 8-10, 2018, by the conference scientific committee. We would also like to thank the anonymous reviewers for comments that greatly improved the manuscript.

References

- Barr, S. & Charusiri, P. (2011). Volcanic rocks. *The Geology of Thailand*, 415-439.
- Barr, S. M., & Cooper, M. A. (2013). Late Cenozoic basalt and gabbro in the subsurface in the Phetchabun Basin, Thailand: Implications for the Southeast Asian Volcanic Province. *Journal of Asian Earth Sciences*, 76, 169-184. doi:10.1016/j.jseas.2013.01.013
- Barr, S. M., Tantisukrit, C., Yaowanoyothin, W., & Mac Donald, A. S. (1990). Petrology and tectonic implication of Upper Paleozoic volcanic rocks of the Chiang Mai Belt, Northern Thailand. *Journal of Southeast Asian Earth Sciences*, 4(1), 37-47. doi:10.1016/0743-9547(90)90023-7
- Blakely, R. J. (1996). *Potential theory in gravity and magnetic applications*. New York, NY: Cambridge University Press.
- Chaturongkawanich, S., Soponpongipat, P., & Chuaviroj, S. (1984). Geological investigation in geothermal development. *Proceeding of the Conference on Applications of Geology and National Development*, Bangkok, Thailand. 67-74.
- Department of Mineral Resources (2003). *Groundwater well data in Chiang Mai province* (Internal report). Bangkok, Thailand: Author.
- Department of Mineral Resources (2007). *Geological map of Thailand, 1:250,000*. Bangkok, Thailand: Author.
- Department of Mineral Resources (2015). *The regional gravity data in northern Thailand* (Unpublished). Bangkok, Thailand: Author.
- Everett, M. E. (2013). *Near-surface applied geophysics*. New York, NY: Cambridge University Press.
- Hara, H., Kunii, M., Miyake, Y., Hisada, K., Kamata, Y., Ueno, K., . . . Charusiri, P. (2017). Sandstone provenance and U-Pb ages of detrital zircons from Permian-Triassic forearc sediments within the Sukhothai Arc, northern Thailand: record of volcanic arc evolution in response to Paleo-Tethys subduction. *Journal of Asian Earth Sciences*, 146, 30-55. doi:10.1016/j.jseas.2017.04.021
- Hatch, D., Kiattiwongchai, T., Wisedsind, W., Boonnop, N., & Kwan, K. (1994). *Creation of nationwide geophysical grids of Thailand, An unpublished technical report for the nationwide data compilation project*.
- Loke, M. H., (2018). *Tutorial: 2-D and 3-D electrical imaging surveys*. Retrieved from <http://www.geotomosoft.com>.
- Metcalf, I. (2017). Tectonic evolution of Sundaland. *Bulletin of the Geological Society of Malaysia*, 63, 27-60. doi:10.7186/bgsm63201702
- Miller, R. D., Xia, J., Park, C. B., & Ivanov, J. M. (1999). Multichannel analysis of surface waves to map bedrock, Kansas Geological Survey. *The Leading Edge*, 18, 1392-1396.
- Park Seismic LLC. (2018). *Multichannel analysis of surface waves*. Retrieved from <http://www.masw.com>.
- Park, C. B., Miller, R. D., & Xia, J. (1998). Imaging dispersion curves of surface waves on multi-channel record. *The 68th Annual International Meeting Society of Exploration Geophysicists, Expanded Abstracts*, 1377-1380.
- Park, C. B., Miller, R. D., & Xia, J. (1999). Multichannel analysis of surface waves. *Geophysics*, 64, 800-808.
- Phajuy, B., Panjasawatwong, Y., & Osataporn, P. (2005). Preliminary geochemical study of volcanic rocks in the Pang Mayao area, Phrao, Chiang Mai, northern Thailand: Tectonic setting of formation. *Journal of Asian Earth Sciences*, 24(6), 765-776. doi:10.1016/j.jseas.2004.06.001

- Telford, W. M., Geldart, L. P., & Sheriff, R. E. (1990). *Applied geophysics*. New York, NY: Cambridge University Press.
- Wang, Y., He, H., Zhang, Y., Srithai, B., Feng, Q., Cawood, P. A. & Fan, W. (2017). Origin of Permian OIB-like basalts in NW Thailand and implications on the Paleotethyan Ocean. *Lithos*, 274-275, 93-105. doi: 10.1016/j.lithos.2016.12.021
- Wattananikorn, K., Beshir, J. A., & Nochaiwong, A. (1995). Gravity interpretation of Chiang Mai Basin, norther Thailand: Concentrating on Ban Thung Sieo area. *Journal of Southeast Asian Earth Science*, 12, No. 1-2, 53-64. doi:10.1016/0743-9547(95)00022-4
- Xia, J., Miller, R. D., & Park, C. B. (1999). Estimation of near-surface shear-wave velocity by inversion of Rayleigh wave. *Geophysics*, 64, 691-700.
- Yilmaz, O., & Doherty, S. M. (2001). *Seismic data analysis: Processing, inversion, and interpretation of seismic data (Volume 1)*. Tulsa, OK: Society of Exploration Geophysicists.